

Cyclic Trinuclear and Chain of Cyclic Trinuclear Copper(II) Complexes Containing a Pyramidal $\text{Cu}_3\text{O}(\text{H})$ Core. Crystal Structures and Magnetic Properties of $[\text{Cu}_3(\mu_3\text{-OH})(\text{aaat})_3(\text{H}_2\text{O})_3](\text{NO}_3)_2 \cdot \text{H}_2\text{O}$ [aaat = 3-Acetylamino-5-amino-1,2,4-triazolate] and $\{[\text{Cu}_3(\mu_3\text{-OH})(\text{aat})_3(\mu_3\text{-SO}_4)] \cdot 6\text{H}_2\text{O}\}_n$ [aat = 3-Acetylamino-1,2,4-triazolate]: New Cases of Spin-Frustrated Systems

Sacramento Ferrer,^{*,†} Francesc Lloret,[†] Ignacio Bertomeu,[†] Gloria Alzuet,[†] Joaquín Borrás,[†] Santiago García-Granda,^{‡,§} Malva Liu-González,^{||} and Jaap G. Haasnoot[⊥]

Departament de Química Inorgànica, Universitat de València, 46100 Burjassot, Valencia, Spain, Departamento de Química Física y Analítica, Universidad de Oviedo, 33006 Oviedo, Spain, Departamento de Termología, Universitat de València, 46100 Burjassot, Valencia, Spain, and Leiden Institute of Chemistry, Gorlaeus Laboratories, Leiden University, P.O. Box 9502, 2300 RA Leiden, The Netherlands

Received March 7, 2002

New copper(II) complexes of the cyclic trinuclear type with 1,2,4-triazole ligands, $[\text{Cu}_3(\mu_3\text{-OH})(\text{aaat})_3(\text{H}_2\text{O})_3](\text{NO}_3)_2 \cdot \text{H}_2\text{O}$ [Haaat = 3-acetylamino-5-amino-1,2,4-triazole] (**1**) and $\{[\text{Cu}_3(\mu_3\text{-OH})(\text{aat})_3(\mu_3\text{-SO}_4)] \cdot 6\text{H}_2\text{O}\}_n$ [Haat = 3-acetylamino-1,2,4-triazole] (**2**), have been prepared and characterized by X-ray crystallography and magnetic measurements. Compound **1**, the first reported with the ligand (H)aaat, consists of discrete trinuclear cations, associated NO_3^- anions and lattice water molecules. Compound **2** consists of unusual chains of trinuclear units with a tridentate sulfato group linking the trimeric units and water molecules stabilizing the crystal lattice. In both complexes, **1** and **2**, the trinuclear $[\text{Cu}_3(\text{OH})\text{L}_3]$ unit contains a pyramidal $\text{Cu}_3\text{-}\mu_3\text{OH}$ core, and an almost flat Cu_3N_6 ring formed by the N,N-bridging triazolato groups. The $\text{Cu}\cdots\text{Cu}'$ intratrimeric distances are 3.35–3.37–3.39 Å in **1** and 3.34–3.34–3.36 Å in **2**. The copper atoms are five-coordinated with a distorted square-pyramidal geometry. Magnetic measurements have been performed in the 1.9–300 K temperature range. In the high-temperature region ($T > 90$ K), experimental data could be satisfactorily reproduced by using an isotropic exchange model, $H = -J(S_1S_2 + S_2S_3 + S_1S_3)$, with $J = -194.6 \text{ cm}^{-1}$ and $g = 2.08$ for **1**, and $J = -185.1 \text{ cm}^{-1}$ and $g = 2.10$ for **2**. The magnitude of the antiferromagnetic exchange in both complexes is discussed on the basis of their structural features by comparison with reported N,N-peripherally bridged trinuclear systems. In order to fit the experimental magnetic data at low temperature, an antisymmetric exchange term, $H_{\text{AS}} = G(S_1 \times S_2 + S_2 \times S_3 + S_1 \times S_3)$, had to be introduced, with $G = 27.8$ (**1**) and 31.0 (**2**) cm^{-1} . Crystal data: $\text{C}_{12}\text{H}_{27}\text{Cu}_3\text{N}_{17}\text{O}_{14}$ (**1**) (MW = 824.13) crystallizes in the triclinic space group, $P\bar{1}$, $Z = 2$, with the cell dimensions $a = 8.852(2)$ Å, $b = 11.491(3)$ Å, $c = 15.404(3)$ Å, $\alpha = 70.43(3)^\circ$, $\beta = 75.11(2)^\circ$, $\gamma = 88.43(2)^\circ$, and $V = 1423.8(5)$ Å³, $D_{\text{calcd}} = 1.922 \text{ g cm}^{-3}$; the final agreement values were $R1 = 0.0822$ and $wR2 = 0.2300$ for 4989 unique reflections. $\text{C}_{12}\text{H}_{28}\text{Cu}_3\text{N}_{12}\text{O}_{14}\text{S}$ (**2**) (MW = 787.14) crystallizes in the triclinic space group, $P\bar{1}$, $Z = 2$, with the cell dimensions $a = 7.146(6)$ Å, $b = 14.26(1)$ Å, $c = 15.35(2)$ Å, $\alpha = 109.0(9)^\circ$, $\beta = 93.6(9)^\circ$, $\gamma = 99.5(7)^\circ$, and $V = 1448(2)$ Å³, $D_{\text{calcd}} = 1.806 \text{ g cm}^{-3}$; the final agreement values were $R1 = 0.0628$ and $wR2 = 0.1571$ for 3997 "observed" reflections.

Introduction

It is well-known that the substituted 1,2,4-triazole ligands can bridge metal ions through the N1,N2-coordination mode

* To whom correspondence may be addressed. E-mail: Sacramento.Ferrer@uv.es.

† Departament de Química Inorgànica, Universitat de València.

to afford polynuclear compounds.¹ Particularly, two series of compounds, one of dimers with a planar double-triazole

‡ Address correspondence pertaining to crystallographic studies to this author.

§ Universidad de Oviedo.

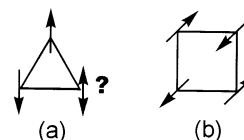
|| Departamento de Termología, Universitat de València.

⊥ Leiden University.

bridge,² and another of linear trinuclear compounds mostly with a triple triazole bridge,^{3,4} have been widely described. Several studies dealing with magnetostructural correlations for the dinuclear copper(II) systems,² and with interesting spin-crossover behavior in the case of the linear trinuclear iron(II) compounds,⁴ have been carried out.

Examples of cyclic trinuclear complexes obtained with 1,2,4-triazole derivatives are, however, very rare.^{5–7} As a part of our search focused on transition metal(II) compounds containing these *N1,N2*-1,2,4-triazole bridges, we previously reported three trinuclear Cu(II) complexes of the *triangular* type, with formula $[\text{Cu}_3(\mu_3\text{-OH})(\text{aat})_3\text{A}(\text{H}_2\text{O})_2]\text{A}\cdot(\text{H}_2\text{O})_x$ [$\text{A} = \text{NO}_3, \text{CF}_3\text{SO}_3, \text{ClO}_4; x = 0, 2$], where Haat = 3-acetyl-amino-1,2,4-triazole.⁷ These three compounds, with strong antiferromagnetic interaction, showed almost equal *J* constants (values from -190 to -198 cm^{-1}) in spite of clear differences in coplanarity of the ligand planes. With the aim of going more deeply into these $\{\text{Cu}_3(\mu_3\text{-O})(\text{N-N})_3\}$ systems, we have undertaken the study of new triangular copper(II) complexes. In this work we describe the synthesis, X-ray structure, and properties of two related cyclic trimeric compounds: $[\text{Cu}_3(\mu_3\text{-OH})(\text{aaat})_3(\text{H}_2\text{O})_3](\text{NO}_3)_2\cdot\text{H}_2\text{O}$ (**1**) (where Haaat = 3-acetyl-amino-5-amino-1,2,4-triazole) and $\{[\text{Cu}_3(\mu_3\text{-OH})(\text{aat})_3(\mu_3\text{-SO}_4)]\cdot 6\text{H}_2\text{O}\}_n$ (**2**). This last compound contains a tris-monodentate sulfato group which connects trimeric units thus yielding chains of trimers. As far as we know, there is only one similar case in the literature, the compound $[\text{Cu}_3(\mu_3\text{-OH})(\text{pz})_3(\text{Hpz})_2(\mu_3\text{-NO}_3)(\text{NO}_3)]\cdot\text{H}_2\text{O}$ (Hpz = pyrazole),⁸ with a nitrate group bridging the trimers.

Scheme 1



The encouragement for the synthesis of trinuclear copper complexes and for the study of their physical and chemical properties is the recent knowledge that blue multicopper oxidases⁹ (e.g., ascorbate oxidase and laccase) contain a triangular unit of copper atoms. In addition, there is a clear interest on cyclic-trinuclear metal complexes¹⁰ because these systems can be regarded as *geometrically frustrated* and offer the opportunity to test magnetic exchange models.¹¹ In fact, geometrically frustrated antiferromagnetic compounds have attracted much attention over the past few years due to their propensity to adopt unusual, even exotic magnetic ground states which remain poorly understood.¹² Toulouse¹³ is credited with introducing the general concept of magnetic frustration, a term applied to the situation wherein a large fraction of magnetic sites in a lattice is subject to competing or contradictory constraints. When frustration arises purely from the geometry or topology of the lattice, it is termed geometric frustration. The canonical example is any lattice based on an equilateral triangular “plaquette”, such as that of Scheme 1a, which depicts the situation for the three nearest neighbor spins. The *isotropic Hamiltonian* for the interaction between any two spins can be written as the scalar product of the spin operators: $\hat{H} = -\sum_{i,j} J_{ij} \hat{S}_i \cdot \hat{S}_j$; therefore the energy is minimized for collinear (parallel or antiparallel) spin alignments. If J_{ij} is negative, which favors the antiparallel (antiferromagnetic) correlation, and J_{ij} is equal for all nearest neighbor pairs, then only two of the three spin constraints can be satisfied simultaneously, i.e., the system is geometrically frustrated. In contrast, the situation of a square planar “plaquette”, shown in Scheme 1b, is clearly not

- (1) Recent examples with numerous references: (a) Koolnaar, J. J. A.; de Heer, M.; Kooijman, H.; Spek, A. L.; Schmitt, G. M.; Ksenofontov, V.; Gütllich, P.; Haasnoot, J. G.; Reedijk, J. *Eur. J. Inorg. Chem.* **1999**, 881. (b) Garcia, Y.; van Koningsbruggen, P. J.; Kooijman, H.; Spek, A. L.; Haasnoot, J. G.; Kahn, O. *Eur. J. Inorg. Chem.* **2000**, 307. (c) Haasnoot, J. G. *Coord. Chem. Rev.* **2000**, 200–202, 131.
- (2) (a) Slangen, P. M.; van Koningsbruggen, P. J.; Haasnoot, J. G.; Jansen, J.; Gorter, S.; Reedijk, J.; Kooijman, H.; Smeets, W. J. J.; Spek, A. L. *Inorg. Chim. Acta* **1993**, 212, 289. (b) Slangen, P. M.; van Koningsbruggen, P. J.; Goubitz, K.; Haasnoot, J. G.; Reedijk, J. *Inorg. Chem.* **1994**, 33, 1121. (c) Ferrer, S.; van Koningsbruggen, P. J.; Haasnoot, J. G.; Reedijk, J.; Kooijman, H.; Spek, A. L.; Lezama, L.; Arif, A. M.; Miller, J. S. *J. Chem. Soc., Dalton Trans.* **1999**, 4269.
- (3) (a) Vos, G.; Haasnoot, J. G.; Verschoor, G. C.; Reedijk, J.; Schaminee, P. E. L. *Inorg. Chim. Acta* **1985**, 105, 31. (b) Vreugdenhil, W.; Haasnoot, J. G.; Schoondergang, M. F. J.; Reedijk, J. *Inorg. Chim. Acta* **1987**, 130, 235. (c) Antolini, L.; Fabretti, A. C.; Gatteschi, D.; Giusti, A.; Sessoli, R. *Inorg. Chem.* **1990**, 29, 143. (d) Antolini, L.; Fabretti, A. C.; Gatteschi, D.; Giusti, A.; Sessoli, R. *Inorg. Chem.* **1991**, 30, 4858. (e) van Koningsbruggen, P. J.; Haasnoot, J. G.; Vreugdenhil, W.; Reedijk, J.; Kahn, O. *Inorg. Chim. Acta* **1995**, 239, 5. (f) Liu, J.; Song, Y.; Yu, Zhi; Zhuang, J.; Huang, X.; You, X. *Polyhedron* **1999**, 18, 1491. (g) Liu, J.; Fu, D.; Zhuang, J.; Duan, C.; You, X. *J. Chem. Soc., Dalton Trans.* **1999**, 2337.
- (4) (a) Thomann, M.; Kahn, O.; Guilhem, J.; Varret, F. *Inorg. Chem.* **1994**, 33, 2433. (b) Kolnaar, J. J. A.; van Dijk, G.; Kooijman, H.; Spek, A. L.; Ksenofontov, V. G.; Gütllich, P.; Haasnoot, J. G.; Reedijk, J. *Inorg. Chem.* **1997**, 36, 2433. (c) Garcia, Y.; van Koningsbruggen, P. J.; Lapouyade, R.; Fourmès, L.; Rabardel, L.; Kahn, O.; Ksenofontov, V.; Levchenko, G.; P. Gütllich, P. *Chem. Mater.* **1998**, 10, 2426. (d) Roubeau, O.; Gómez, J. M. A.; Balskus, E.; Kolnaar, J. J. A.; Haasnoot, J. G.; Reedijk, J. *New J. Chem.* **2001**, 25, 144.
- (5) Vreugdenhil, W. Ph.D. Thesis, Leiden University, The Netherlands, 1987.
- (6) Virovets, A. V.; Podberezskaya, N. V.; Lavrenova, L. G. *J. Struct. Chem.* **1997**, 38, 441.
- (7) Ferrer, S.; Haasnoot, J. G.; Reedijk, J.; Müller, E.; Biagini Cingi, M.; Lanfranchi, M.; Manotti Lanfredi, A. M.; Ribas, J. *Inorg. Chem.* **2000**, 39, 1859.

- (8) (a) Hulsbergen, F. B.; ten Hoedt, R. W. M.; Verschoor, J.; Reedijk, J.; Spek, A. L. *J. Chem. Soc., Dalton Trans.* **1983**, 539. (b) Sakai, K.; Yamada, Y.; Tsubomura, T.; Yabuki, M.; Yamaguchi, M. *Inorg. Chem.* **1996**, 35, 522. The compound described in this paper presents a trinuclear unit identical to that of the compound of ref 8a, but one nitrate group links the trimeric units in pairs; so, the compound of ref 8b can be considered a hexamer, not a chain. Its magnetic properties have not been studied.
- (9) Messerschmidt, A. *Struct. Bonding (Berlin)* **1998**, 90, 37–68 and references therein.
- (10) (a) Chaudhuri, P.; Karpenstein, I.; Winter, M.; Butzlaff, C.; Bill, E.; Trautwein, A. X.; Flörke, U.; Haupt, H.-J. *J. Chem. Soc., Chem. Commun.* **1992**, 321. (b) Cole, A. P.; Root, D. E.; Mukherjee, P.; Solomon, E. I.; Stack, T. D. P. *Science* **1996**, 273, 1848. (c) Frey, S. T.; Sun, H. H. J.; Murthy, N. N.; Karlin, K. D. *Inorg. Chim. Acta* **1996**, 242, 329. (d) Spiccia, L.; Graham, B.; Hearn, M. T. W.; Lazarev, G.; Moubaraki, B.; Murray, K. S.; Tiekink, E. D. *J. Chem. Soc., Dalton Trans.* **1997**, 4089.
- (11) (a) *Magnetic Molecular Materials*; Gatteschi, D., Kahn, O., Müller, J. S., Palacio, F., Eds.; Kluwer Academic: Dordrecht, The Netherlands, 1991. (b) Kahn, O.; Pei, Y.; Yournaux, Y. In *Inorganic Materials*; Bruce, D. W., O'Hare, O., Eds.; John Wiley & Sons: Chichester, U.K., 1992. (c) Kahn, O. *Molecular Magnetism*; VCH Publishers: New York, 1993. (d) *Molecule-Based Magnetic Materials: Theory, Techniques, and Applications*; Turnbull, M. M., Sugimoto, T., Thompson, L. K., Eds.; ACS Symposium Series 644; American Chemical Society: Washington, DC, 1996.
- (12) Greedan, J. E. *J. Mater. Chem.* **2001**, 11, 37.
- (13) Toulouse, C. *Commun. Phys.* **1977**, 2, 115.

frustrated under the same constraints. In order to interpret the magnetic properties of these frustrated systems it is necessary to go beyond the framework of the above isotropic exchange model and to introduce an *antisymmetric exchange interaction*.

The exchange interactions for a pair of paramagnetic ions with spins S_A and S_B can be described with the Hamiltonian $\hat{H}_{\text{ex}} = \hat{S}_A \mathbf{J}_{AB} \hat{S}_B$, where \mathbf{J}_{AB} is a 3×3 tensor that contains the relevant exchange parameters. This \mathbf{J}_{AB} tensor can be decomposed into a scalar parameter, J (which describes the isotropic exchange and is generally the dominating term), a traceless symmetric tensor, \mathbf{D}_{AB} (which describes the anisotropic exchange), and an antisymmetric tensor.¹⁴ The antisymmetric exchange term, defined by the expression $\mathbf{G}_{AB}[S_A \times S_B]$, where \mathbf{G}_{AB} is an antisymmetric vector ($\mathbf{G}_{AB} = -\mathbf{G}_{BA}$), was introduced phenomenologically by Dzyaloshinsky to explain the weak ferromagnetism of α -Fe₂O₃.¹⁵ The microscopic meaning of \mathbf{G}_{AB} was introduced by Moriya.¹⁶ Therefore, the corresponding operator is usually termed Dzyaloshinsky–Moriya antisymmetric (AS) interaction. For systems without orbital degeneracy (such as Cu(II) ions), the AS exchange arises in second order from an interplay between spin–orbit coupling and isotropic exchange. Moriya formulated rules to specify the direction of \mathbf{G}_{AB} for certain symmetries; it vanishes when an inversion center is present in the pair A–B.

The $-\hat{J} \hat{S}_A \hat{S}_B$ term leads to parallel or antiparallel alignment of S_A and S_B , depending on the nature of magnetic interaction (ferro- or antiferromagnetic), whereas the $\mathbf{G}_{AB}[S_A \times S_B]$ term tends to orient the spins perpendicular to each other and perpendicular to \mathbf{G}_{AB} .¹⁷ These competitive interactions between both terms yield a nonalignment of S_A and S_B (spin canting). In fact, the antisymmetric exchange has been frequently claimed for magnetically ordered states of extended lattices where it gives rise to the phenomenon of spin canting.¹⁸ Information about \mathbf{G}_{AB} values for isolated complexes is, however, very scarce.

Tsukerblat and co-workers¹⁹ have studied extensively the consequences of the antisymmetric exchange on the electronic properties of trinuclear complexes, providing the first experimental observation of this type of interaction in a transition-metal complex. These authors considered the trinuclear complex [Cu₃(μ_3 -OH)(pyridine-2-aldoxime)₃](SO₄)·10.5H₂O, with a trigonal symmetry, similar to that of complexes **1** and **2**, and obtained a value of 6 cm⁻¹ for its G parameter.²⁰ Previously, Lines et al. analyzed the magnetic susceptibility data of the tetrameric copper complex [Cu₄(μ_4 -O)(triphenylphosphine oxide)₄Cl₆] assuming a G value

of 28 cm⁻¹.²¹ However, Black et al. interpreted the EPR spectra of this compound without taking into account the antisymmetric exchange, thus introducing a conflict with the susceptibility data.²²

More recently, Nishimura et al. explained anomalous g -value shifts of the trimeric compound [Cr₃(μ_3 -O)(acetato)₆(H₂O)₃](NO₃)·2H₂O, by assuming $G = 0.62$ cm⁻¹.²³ Rakitin et al. deduced the value $G = 1.4$ cm⁻¹ for the complex [Fe₃(μ_3 -O)(propanoato)₆(H₂O)₃]Cl·5H₂O from EPR spectra.²⁴ Gatteschi et al. obtained values of G in the range 5–9 cm⁻¹ for equilateral triangles of V(IV).²⁵ Münck et al. studied the Mössbauer spectra of the triiron cluster [3Fe–4S] of ferredoxin II,²⁶ the antiferromagnetic coupled diiron cluster of the methane monooxygenase,²⁷ and a synthetic Fe(III) binuclear complex,²⁸ and they showed the occurrence of antisymmetric exchange in all these systems, with G values of 0.4, 1.5, and 2.2 cm⁻¹, respectively.

In the present work, the magnetic behavior of compounds **1** and **2**, which can be regarded as geometrically frustrated systems, is studied by considering that the antisymmetric exchange interaction is operating. The corresponding calculations and results are reported.

Experimental Section

Synthesis of the Ligands. The ligands Haaat and Haat have been synthesized by adaptation of the method described by van den Bos.²⁹

Synthesis of [Cu₃(μ_3 -OH)(aaat)₃(H₂O)₃](NO₃)₂·H₂O (1**).** Solid Haaat (3 mmol) was dissolved in an aqueous solution of copper(II) nitrate (3 mmol in 40 mL) (molar ratio Haaat:Cu = 1:1) with continuous stirring and slight heating. Then 0.05 mL of ethanediamine (99% pure, Merck quality) was added. The resulting dark green solution was allowed to slowly evaporate at room temperature. After ca. 3 months, from a thick dark suspension single crystals of **1**, dark green with shape almost cubic, were isolated on filter paper and washed with water. (Yield: ca. 70%.) *Note:* Green crystals with IR spectrum identical to that of **1** could be obtained by adding NH₃ instead of ethanediamine; these crystals were analyzed by elemental analysis, and the experimental results were also in agreement with the values calculated for the formula of **1**.

Synthesis of {[Cu₃(μ_3 -OH)(aat)₃(μ_3 -SO₄)·6H₂O]_n (2**).** An aqueous solution of CuSO₄·5H₂O (0.250 g in 20 mL) (1 mmol) was mixed with an aqueous suspension of Haat (0.126 g in 20 mL) (1 mmol) (molar ratio Haat:Cu = 1:1). After a few minutes of stirring the ligand was dissolved. The resulting solution was allowed to stand. Within ca. 3 h. a powdered light blue precipitate was obtained, which was filtered off and washed with water. (Yield: ca. 80%). Single crystals of **2** were obtained as follows: A 20 mL aqueous solution of copper(II) bromide (0.223 g) (1 mmol)

(14) Bencini, A.; Gatteschi, D. *Electron Paramagnetic Resonance of Exchange Coupled Systems*; Springer-Verlag: Berlin, Heidelberg, 1990.

(15) Dzyaloshinski, I. *J. Phys. Chem. Solids* **1958**, *4*, 241.

(16) Moriya, T. *Phys. Rev.* **1960**, *120*, 91.

(17) Erdős, P. *J. Phys. Chem. Solids* **1966**, *27*, 1705.

(18) Coffey, D.; Bedell, K. S.; Trugman, S. A. *Phys. Rev. B* **1990**, *42*, 6509.

(19) Tsukerblat, B. S.; Belinskii, M. I.; Fainzil'berg, V. E. *Sov. Sci. Rev. B (Engl. Transl.)* **1987**, *9*, 339.

(20) Tsukerblat, B. S.; Kuyavskaya, B. Y.; Belinskii, M. I.; Ablov, A. V.; Novotortsev, V. M.; Kalinnikov, V. T. *Theor. Chim. Acta* **1975**, *38*, 131.

(21) Lines, M. E.; Ginsberg, A. P.; Martin, R. L. *Phys. Rev. Lett.* **1972**, *28*, 684.

(22) Black, T. D.; Rubins, R. S.; De, D. K.; Dickson, R. C.; Baker, W. A., Jr. *J. Chem. Phys.* **1984**, *80*, 4620.

(23) Nishimura, H.; Date, M. *J. Phys. Soc. Jpn.* **1985**, *54*, 395.

(24) Rakitin, Y. V.; Yablokov, Y. V.; Zelentsov, V. V. *J. Magn. Reson.* **1981**, *43*, 288.

(25) Gatteschi, D.; Sessoli, R.; Plass, W.; Müller, A.; Krickemeyer, E.; Meyer, J.; Sölter, D.; Adler, P. *Inorg. Chem.* **1996**, *35*, 1926.

(26) Sanakis, Y.; Macedos, A. L.; Moura, I.; Moura, J. J. G.; Papaefthymiou, V.; Münck, E. *J. Am. Chem. Soc.* **2000**, *122*, 11855.

(27) Kauffmann, K. E.; Popescu, C. V.; Dong, Y.; Lipscomb, J. D. Que, L., Jr.; Münck, E. *J. Am. Chem. Soc.* **1998**, *120*, 8739.

(28) Griffit, J. S. *Struct. Bonding (Berlin)* **1972**, *10*, 87.

(29) van den Bos, B. G. *Recl. Trav. Chim. Pays-Bas.* **1960**, *79*, 836.

containing a very small amount of copper(II) sulfate (2×10^{-4} mmol) was mixed with an aqueous suspension of Haat (0.252 g in 20 mL) (2 mmol) (molar ratio Haat:Cu = 2:1) and with 0.02 mL of concentrated ammonia. From the resulting solution a few blue prismatic single crystals appeared in ca. 12 days. The IR spectrum of crystals was identical to that of the powdered product. The experimental X-ray powder diagram of the powdered sample was coincident in the main peaks with the theoretical one obtained from the single-crystal X-ray data (by using the program PowderCell 2.0 for Windows, G. Norze and W. Kraus, 1998).

Analysis. Calcd for $C_{12}H_{27}Cu_3N_{17}O_{14}$ (**1**) (MW = 824.13): C, 17.5; H, 3.3; N, 28.9. Found: C, 17.4; H, 3.3; N, 29.2. Calcd for $C_{12}H_{28}Cu_3N_{12}O_{14}S_1$ (**2**) (MW = 787.14): C, 18.3; H, 3.6; N, 21.4; S, 4.1. Found: C, 18.3; H, 3.4; N, 20.7; S, 3.9. Single crystals of compound **2** were not analyzed other than by the X-ray analysis, shown below.

Spectroscopy. $\tilde{\nu}_{\max}/\text{cm}^{-1}$ for Haat: $[\nu(\text{N-H})_{\text{NH}_2}]$ 3427, 3399m–s(split); $[\nu(\text{C=O})]$ 1713s; $[\nu(\text{C=N}) + \delta(\text{N-H})]$ 1643s, 1572s. $\tilde{\nu}_{\max}/\text{cm}^{-1}$ for Haat: already described.⁷

λ_{\max}/nm (solid sample) for **1**: 685. $\tilde{\nu}_{\max}/\text{cm}^{-1}$ for **1**: $[\nu(\text{O-H})_{\text{OH},\text{H}_2\text{O}} + \nu(\text{N-H})_{\text{NH}_2}]$ 3452m, 3321w; $[\nu(\text{C=O})]$ 1636s; $[\nu(\text{C=N}) + \delta(\text{N-H})]$ 1595s, 1501s; $[\nu_{\text{asym}}(\text{NO}_3)]$ 1384vs, 1288w; $[\nu_{\text{sym}}(\text{NO}_3)]$ 1104m.

λ_{\max}/nm (solid sample) for **2**: 675. $\tilde{\nu}_{\max}/\text{cm}^{-1}$ for **2**: $[\nu(\text{O-H})_{\text{OH},\text{H}_2\text{O}}]$ 3399m(broad); $[\nu(\text{C=O})]$ 1629s; $[\nu(\text{C=N}) + \delta(\text{N-H})]$ 1587s, 1517s; $[\nu_3(\text{SO}_4)]$ 1140s–1110s; $[\nu_3(\text{SO}_4)]$ 1066m–w; $[\nu_4(\text{SO}_4)]$ 621m.

Physical Measurements. Elemental analyses were performed with a Carlo Erba instrument at the Universidad Politécnic de Valencia, Spain. Infrared spectra were obtained with a Satellite FTIR Mattson spectrophotometer in the region 4000–400 cm^{-1} as KBr pellets. Ligand field spectra were registered in the region 800–200 nm on a Shimadzu 2101PC UV–vis spectrophotometer, by the use of the diffuse-reflectance technique, with Nujol. Magnetic susceptibility and magnetization measurements were carried out in the 1.9–300 K temperature range with a Quantum Design MPMS5 SQUID magnetometer. Diamagnetic corrections were estimated from Pascal's constants. Experimental susceptibilities were also corrected for the temperature independent paramagnetism ($-60 \times 10^{-6} \text{ cm}^3 \text{ mol}^{-1}$ per Cu(II)) and for the magnetization of the sample holder.

Crystallography. X-ray Data Collection, Structure Determination, and Refinement of Complexes 1 and 2. The crystallographic data for **1** and **2** are summarized in Table 1. A dark green and blue prismatic crystals, respectively, were selected. Throughout the experiment Mo K α was used with a graphite crystal monochromator on a Nonius CAD-4 single-crystal diffractometer ($\lambda = 0.71073 \text{ \AA}$). The unit cell dimensions were determined from the angular settings of 25 reflections with θ between 1.00° and 10.13° for **1** and between 10° and 13° for **2** and refined with CAD4 software.³⁰ The space groups were determined to be triclinic $P\bar{1}$ from structure determination. Reflections were measured using the ω – 2θ scan technique and variable scan rate with a maximum scan time of 60 s per reflection. On all reflections of structure **2** profile analysis was performed.³¹ One absorption correction was made for structure **1** by using the semiempirical PSISCANS method.³² The intensity of the primary beam was checked throughout the data collection by monitoring three standard reflections every 60 min.

(30) CAD4 Software; Enraf-Nonius: Delft, The Netherlands, 1996.

(31) Strel'tsov, V. A.; Zavodnik, V. E. *PROFIT—Profile Fitting Data Reduction. Sov. Phys. Crystallogr.* **1990**, *35*, 281.

(32) North, A. C. T.; Phillips, D. C.; Mathews, F. S. *Acta Crystallogr.* **1968**, *A24*, 351.

Table 1. Crystal Data and Structure Refinement for Compounds **1** and **2**^a

	1	2
empirical formula	$C_{12}H_{27}Cu_3N_{17}O_{14}$	$C_{12}H_{28}Cu_3N_{12}O_{14}S$
fw	824.13	787.14
temp (K)	293(2)	293(2)
wavelength (\AA)	0.71073	0.71073
cryst syst, space group	triclinic, $P\bar{1}$	triclinic, $P\bar{1}$
unit cell dimens		
<i>a</i> (\AA)	8.852(2)	7.146(6)
<i>b</i> (\AA)	11.491(3)	14.26(1)
<i>c</i> (\AA)	15.404(3)	15.35(2)
α (deg)	70.43(3)	109.0(9)
β (deg)	75.11(2)	93.6(9)
γ (deg)	88.43(2)	99.5(7)
vol (\AA^3)	1423.8(5)	1448(2)
Z, calcd density (g/cm ³)	2, 1.922	2, 1.806
abs coeff (mm ⁻¹)	2.315	2.337
<i>F</i> (000)	834	798
cryst size (mm)	$0.20 \times 0.15 \times 0.20$	$0.33 \times 0.26 \times 0.19$
θ range for data collection (deg)	1.00–25.0	1.41–22.98
index ranges	$0 \leq h \leq 10,$ $-13 \leq k \leq 13,$ $-17 \leq l \leq 18$	$-7 \leq h \leq 7,$ $-15 \leq k \leq 14,$ $0 \leq l \leq 16$
reflns collected/unique	4989/4989	4174/3997 [<i>R</i> (int) = 0.045]
refinement meth	full-matrix least-squares on F^2	
data/restraints/params	4989/14/452	3997/0/396
GOF on F^2	1.112	1.041
final <i>R</i> indices [$I > 2\sigma(I)$] (<i>R</i> 1, <i>wR</i> 2)	0.0822, 0.2300	0.0628, 0.1571
<i>R</i> indices (all data) (<i>R</i> 1, <i>wR</i> 2)	0.1130, 0.2872	0.1510, 0.1895
largest diff peak and hole (e \AA^{-3})	1.672 and -1.543	1.654 and -0.604

^a GOF = $[\sum[w(F_o^2 - F_c^2)^2]/(n - p)]^{1/2}$, $R_1 = \sum||F_o| - |F_c||/\sum|F_o|$, $wR_2 = [\sum[w(F_o^2 - F_c^2)^2]/\sum[w(F_o^2)^2]]^{1/2}$, $w = 1/[\sigma^2(F_o^2) + (aP)^2 + bP]$, where $P = [\max(F_o^2, 0) + 2F_c^2]/3$. For **1**: $a = 0.2000$, $b = 0.0000$. For **2**: $a = 0.0997$, $b = 6.1751$.

Lorentz polarization corrections were applied, and then data were reduced to F_o^2 values.³³ The structures were solved respectively using SIR 92³⁴ (**1**) and DIRDIF³⁵ (**2**). Isotropic least-squared refinement on F^2 was made using SHELX93.³⁶ At this stage an empirical absorption correction was applied to structure **2** using XABS2.³⁷ During the final stages of the refinement on F^2 the positional parameters and the anisotropic thermal parameters of the non-H atoms were refined. Some hydrogen atoms were located by Fourier difference synthesis, but most of them were geometrically placed. The final difference Fourier map for **1** showed the highest peak of 1.672 e \AA^{-3} and the deepest hole of -1.54 e \AA^{-3} close to Cu(3), while the same map for **2** showed a peak of 1.67 e \AA^{-3} very close to the sulfur atom; the rest of them were not higher than 0.80 nor deeper than -0.60 e \AA^{-3} . Figure 1, made with ORTEP,³⁸ and Figure 2, made with EUCLID,³⁹ show the atomic numbering schemes. Atomic scattering factors were taken from ref 40. Geometrical calculations were made with PARST.⁴¹

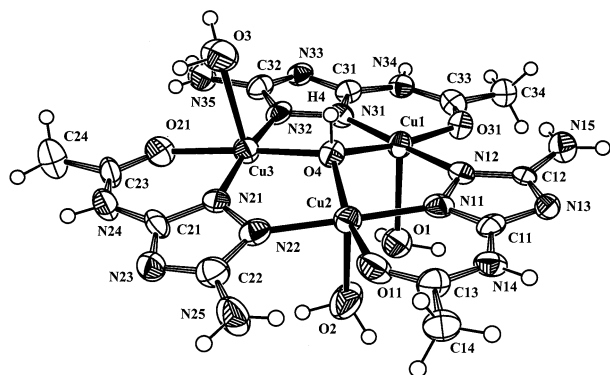
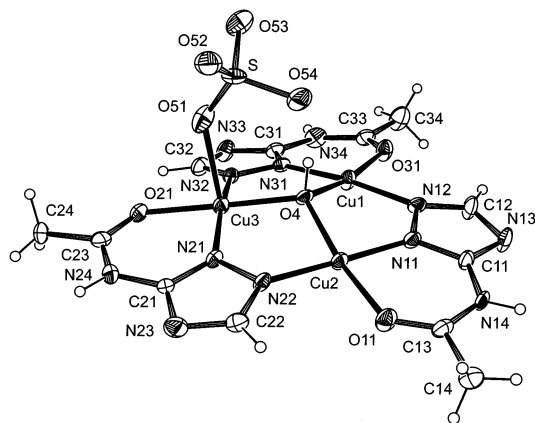
(33) Harms, K.; Wocadlo, S. *XCAD4—CAD4 Data Reduction*; University of Marburg: Marburg, Germany, 1995.

(34) Altomare, A.; Cascarano, G.; Giacovazzo, C.; Guagliardi, A. SIR92—A Program for Crystal Structure Solution. *J. Appl. Crystallogr.* **1993**, *26*, 343.

(35) Beurskens, P. T.; Admiraal, G.; Beurskens, G.; Bosman, W. P.; García-Granda, S.; Gould, R. O.; Smits, J. M. M.; Smykalla, C. *DIRDIF user's guide technical report*; Crystallography Laboratory, University of Nijmegen: Nijmegen, The Netherlands, 1992.

(36) Sheldrick, G. M. *SHELXL93—Program for Crystal Structure Refinement*; Institut für Anorganische Chemie der Universität: Tammanstrasse 4, D-3400 Göttingen, Germany, 1993.

(37) Parkin, S.; Mopezzi, B.; Hope, H. *J. Appl. Crystallogr.* **1995**, *28*, 53.

Figure 1. ORTEP view of **1**.Figure 2. ORTEP view of **2**.

Results and Discussion

Ligands and Complexes. The substituted 1,2,4-triazole derivatives are versatile ligands. Complexes with different nuclearity have been obtained depending on variables such as the nature of the substituents, co-ligands, and anion and the metal–ligand ratio.^{1–4} In this work the coordination properties of the (H)aaat molecule have been tested for the first time. The structure of **1** supports the idea upon the influence of the *length* of the chelating substituent in the way of coordination of the triazole derivative since, in the presence of Cu(II), the (H)aaat [3-acetylamino-5-amino-1,2,4-triazole] affords, as the (H)aat [3-acetylamino-1,2,4-triazole], *cyclic trinuclear* complexes in which the substituted triazole, in the dehydrated form, behaves as a tridentate chelating and bridging ligand, forming with the metal ion six-membered chelating rings.⁷ This situation was also found in the compounds [Cu₃(μ₃-OH)(hppt)₃(A)₂](H₂O)_x [hppt = 3-(2-hydroxyphenyl)-4-phenyl-1,2,4-triazole; A = NO₃, ClO₄, CF₃SO₃, x = 4, 2, 3] described by Vreugdenhil et al.⁵ It must also be indicated that Virovets et al. have reported a cyclic trinuclear copper(II) compound with the ligand 3,5-dimethyl-4-amino-1,2,4-triazole, so with no chelating substituent.⁶

Besides, under different synthesis conditions, the ligand (H)aat forms with Cu(II) mononuclear species.⁴²

On the other hand, similar regular triangular M₃O arrays have been reported for a variety of metals (Ni,^{43a,f} Fe,^{43c,d,f} Mn,^{43b,d} Cr,^{43c,e,f} Cu^{5–8,44–51}) and ligands; frequently they are present in structures which contain N,O (from oximate ligands or nitrito groups) or O,O (from carboxylate groups) peripheral bridges. N,N-Bridged trimeric Cu(II) complexes are not common; only three compounds with the simple pyrazole ligand^{8a,b,51} and the above-mentioned compounds with triazole derivatives^{5–7} have been structurally characterized. With Cu(II) and appropriately substituted 1,2,4-triazole ligands, triangular systems with peripheral N,N bridges can be obtained. Presumably the analogous pyrazole derivatives could also give this type of cluster.

Description of the Structures. The crystal structure of **1** is built up by discrete trinuclear cations, [Cu₃(μ₃-OH)(aaat)₃-(H₂O)₃]²⁺, and two noncoordinated nitrate anions and one lattice water molecule per cation (ORTEP view in Figure 1). This structure is similar to that of the three compounds [Cu₃(μ₃-OH)(aat)₃A(H₂O)₂](H₂O)_x [A = NO₃, CF₃SO₃, ClO₄; x = 0, 2] (**3**, **4**, **5**), obtained with the related (H)aat ligand and reported in a previous paper.⁷

The crystal structure of **2** consists of *chains* of cyclic trinuclear Cu(II) units of formula [Cu₃(μ₃-OH)(aat)₃(μ₃-SO₄)] (ORTEP view in Figure 2). Trimeric [Cu₃(μ₃-OH)(aat)₃]²⁺ entities, of the same type as the cations of **1** and **3–5**, are bridged by one tridentate sulfato group, resulting in a one-dimensional network. Part of the chain is presented in Figure 3. Six noncoordinating water molecules complete the asymmetric unit. As far as we know, only one chain with comparable structure has been described in the literature, that of [Cu₃(μ₃-OH)(pz)₃(Hpz)₂(μ₃-NO₃)(NO₃)]·H₂O, also based on a nine-membered Cu₃N₆ ring but with the ligand pyrazolate [pz] instead of a triazolate derivative and with a nitrate group instead of a sulfato one bridging the trimers.⁸

(38) Farrugia, L. J. ORTEP3 for Windows. *J. Appl. Crystallogr.* **1997**, *30*, 565.

(39) Speck, A. L. The EUCLID package. In *Computational Crystallography*; Sayre, D., Ed.; Clarendon Press: Oxford, 1982.

(40) *International Tables for X-Ray Crystallography*; Hahn, T., Ed.; Kluwer Academic Publishers: Dordrecht, The Netherlands, 1995; Vol. A.

(41) Nardelli, M. *Comput. Chem.* **1983**, *7*, 95.

(42) (a) Virovets, A. V.; Maumov, D. Y.; Lavrenova, L. G.; Bushuev, M. B. *Acta Crystallogr., Sect. C* **1999**, *55*, 9900059. (b) Cingi, M. B.; Lanfredi, A.-M. M.; Tiripicchio, A.; Haasnoot, J. G.; Reedijk, J. *Acta Crystallogr., Sect. C* **1989**, *45*, 601.

(43) (a) Finney, A. J.; Hitchman, M. A.; Raston, C. L.; Rowbottom, G. L.; White, A. H. *Aust. J. Chem.* **1981**, *34*, 2139. (b) Ribas, J.; Albela, B.; Stoeckli-Evans, H.; Christou, G. *Inorg. Chem.* **1997**, *36*, 2352. (c) Anson, C. E.; Bourke, J. P.; Cannon, R. D.; Jayasooriya, U. A.; Molinier, M.; Powell, A. K. *Inorg. Chem.* **1997**, *36*, 1265. (d) Wu, R. W.; Poyraz, M.; Sowrey, F. E.; Anson, C. E.; Wocadlo, S.; Powell, A. K.; Jayasooriya, U. A.; Cannon, R. D.; Nakamoto, T.; Katada, M.; Sano, H. *Inorg. Chem.* **1998**, *37*, 1913. (e) Chaudhuri, P.; Hess, M.; Rentschler, E.; Weyhermuller, T.; Florke, U. *New J. Chem.* **1998**, *22*, 553. (f) Blake, A. B.; Sinn, E.; Yavari, A.; Murray, K. S.; Moubaraki, B. *J. Chem. Soc., Dalton Trans.* **1998**, 45.

(44) Beckett, R.; Hoskins, B. F. *J. Chem. Soc., Dalton Trans.* **1972**, 291.

(45) Ross, P. F.; Murmann, R. K.; Schlemper, E. O. *Acta Crystallogr., Sect. B* **1974**, *B30*, 1120.

(46) Butcher, R. J.; O'Connor, C. J.; Sinn, E. *Inorg. Chem.* **1981**, *20*, 537.

(47) Baral, S.; Chakravorty, A. *Inorg. Chim. Acta* **1980**, *39*, 1.

(48) Agnus, Y.; Louis, R.; Metz, B.; Boudon, C.; Gisselbrecht, J. P.; Gross, M. *Inorg. Chem.* **1991**, *30*, 3155.

(49) (a) Costes, J. P.; Dahan, F.; Laurent, J. P. *Inorg. Chem.* **1986**, *25*, 413. (b) Kriatkowski, M.; Kriatkowski, E.; Olechnowick, D.; Ho, D. M.; Deustch, E. *Inorg. Chim. Acta* **1988**, *150*, 65.

(50) Yang, X.; Zhang, X.; Li, C.; Hu, X.; Jin, D. *Transition Met. Chem.* **2000**, *25*, 174.

(51) Angaroni, M.; Ardizzoia, G. A.; Beringhelli, T.; La Monica, G.; Gatteschi, D.; Masciocchi, N.; Moret, M. *J. Chem. Soc., Dalton Trans.* **1990**, 3305.

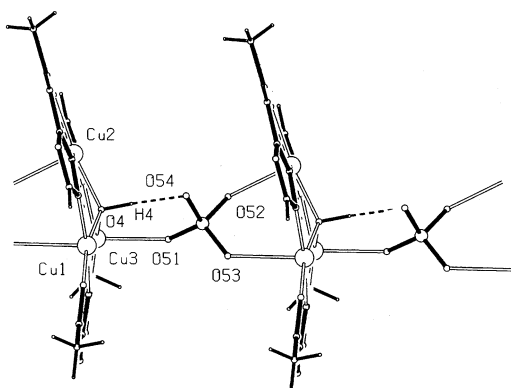


Figure 3. Part of the chain of **2** showing the coordination way of the tridentate sulfate anion.

Relevant bond lengths and angles for **1** and **2** are listed in Table 2. In both **1** and **2**, each trinuclear cluster contains a triangular Cu₃ skeleton (with Cu–Cu edges of 3.35–3.37–3.39 Å (**1**); 3.34–3.34–3.36 Å (**2**)) in which the copper atoms are held together by two bridging systems: (i) the oxygen atom of the central μ_3 -hydroxo group (the Cu–O distances being 1.99, 1.99, and 2.00 Å (**1**); 1.99, 1.99, and 2.01 Å (**2**)) and (ii) the N1,N2-diazinic groups from the triazole rings of three pseudo 3-fold symmetry-related aat(**1**)/aat(**2**) ligands (Cu–N distances ranging from 1.90 to 1.97 Å (**1**); 1.91 to 1.95 Å (**2**)). In the pyramidal Cu₃O group the averaged Cu–O–Cu' angle is 115.4° in **1** and 113.7° in **2**. All these distances and angles are considered normal for these systems.⁷ In both compounds, the hydrogen atom of the OH[−] group within the complex was clearly detectable in a difference Fourier map during the refinement of the X-ray structures. The μ_3 -hydroxo oxygen atom O(4) is bridging *above* the plane defined by the three copper atoms (at 0.435(7) Å in **1**; 0.512(7) Å in **2**), while the three pseudo symmetry-related triazole rings lie *below* (the dihedral angles between the triazole ring planes and the plane through the three Cu atoms are 14.8(2)°, 6.1(2)°, 5.0(2)° in **1**; 19.8(4)°, 12.5(4)°, 6.6(4)° in **2**).

As for the copper environment, in both structures, **1** and **2**, the three copper atoms of the trinuclear entity are five-coordinated with a square-pyramidal (NN'OO' + O'') geometry appreciably distorted (interatomic X–Cu–Y angles in equatorial positions vary from 85.8(3)° to 95.1(3)° (**1**)/87.1(4)° to 94.9(4)° (**2**); the basal plane is occupied by O(μ_3 -OH[−]), N1(triazole), N2'(triazole), and O(carbonyl) atoms. Each copper is displaced from the least-squares plane through the basal atoms in the direction of the apical coordination atom by 0.085(1) Å [Cu(1)], 0.172(2) Å [Cu(2)], and 0.072(2) Å [Cu(3)] in **1**; and by 0.047(2) Å [Cu(1)], 0.080(2) Å [Cu(2)], and 0.091(2) Å [Cu(3)] in **2**.

In **1**, the O atoms on apical positions (at 2.273(9), 2.386(9), and 2.482(3) Å) are afforded by three water molecules. These axial O atoms are trans [Cu(1)], trans [Cu(2)], and cis [Cu(3)] with respect to the H(OH[−]) atom. Furthermore, the three copper atoms tend to the octahedral coordination through a sixth position achieved at the following semi-bonding distances: Cu(1)–N(15^I) = 2.87(2) Å (I: $-x + 1, -y + 1, -z + 1$) (from an amino group of a different trimeric

Table 2. Selected Bond Lengths (Å) and Angles (deg) for **1** and **2**^a

	1	2
Cu(1)–Cu(2)	3.347(2)	3.337(4)
Cu(1)–Cu(3)	3.374(2)	3.364(4)
Cu(2)–Cu(3)	3.393(2)	3.337(5)
Cu(1)–N(12)	1.965(7)	1.941(9)
Cu(1)–N(31)	1.909(7)	1.919(9)
Cu(1)–O(31)	1.995(6)	1.999(8)
Cu(1)–O(4)	1.996(6)	2.009(7)
Cu(1)–O(1) ^b /O(53')	2.482(3)	2.460(10)
Cu(2)–N(22)	1.929(8)	1.955(9)
Cu(2)–N(11)	1.921(8)	1.907(9)
Cu(2)–O(11)	2.020(7)	2.006(9)
Cu(2)–O(4)	1.993(6)	1.993(7)
Cu(2)–O(2)/O(52')	2.273(9)	2.255(10)
Cu(3)–N(32)	1.929(8)	1.948(9)
Cu(3)–N(21)	1.899(8)	1.918(9)
Cu(3)–O(21)	2.024(7)	1.965(8)
Cu(3)–O(4)	1.994(6)	1.994(7)
Cu(3)–O(3)/O(51)	2.386(9)	2.298(10)
S–O(51)		1.380(10)
S–O(52)		1.443(9)
S–O(53)		1.439(9)
S–O(54)		1.564(9)
Cu(1)–O(4)–Cu(2)	114.1(3)	113.0(3)
Cu(1)–O(4)–Cu(3)	116.5(3)	114.4(3)
Cu(2)–O(4)–Cu(3)	115.6(3)	113.6(4)
N(31)–Cu(1)–O(31)	87.7(3)	87.1(4)
N(12)–Cu(1)–O(31)	95.3(3)	94.9(4)
N(12)–Cu(1)–O(4)	88.9(3)	89.5(3)
N(31)–Cu(1)–O(4)	87.7(3)	89.6(3)
N(11)–Cu(2)–O(11)	85.8(3)	87.3(4)
N(22)–Cu(2)–O(11)	94.7(3)	93.7(4)
N(22)–Cu(2)–O(4)	91.1(3)	91.4(3)
N(11)–Cu(2)–O(4)	88.1(3)	87.6(3)
N(11)–Cu(2)–O(2)/O(52')	93.4(3)	94.1(4)
O(11)–Cu(2)–O(2)/O(52')	98.0(4)	98.4(3)
N(22)–Cu(2)–O(2)/O(52')	87.5(3)	86.4(4)
O(4)–Cu(2)–O(2)/O(52')	98.9(4)	89.6(3)
N(21)–Cu(3)–O(21)	87.2(3)	88.1(4)
N(32)–Cu(3)–O(21)	94.2(3)	91.9(4)
N(32)–Cu(3)–O(4)	90.1(3)	91.4(4)
N(21)–Cu(3)–O(4)	88.4(3)	89.3(4)
N(21)–Cu(3)–O(3)/O(51)	95.5(3)	100.6(4)
O(21)–Cu(3)–O(3)/O(51)	87.3(3)	87.8(3)
N(32)–Cu(3)–O(3)/O(51)	93.1(3)	96.5(4)
O(4)–Cu(3)–O(3)/O(51)	93.8(3)	89.5(3)

^a Symmetry transformations used to generate equivalent atoms in **2**: (') $x - 1, y, z$. ^b First atom refers to **1**/second atom refers to **2**.

unity); Cu(2)–O(42) = 2.81(2) Å (from a nitrate); and Cu(3)–O(52^{II}) = 2.83(2) Å (II: $-x + 2, -y + 2, -z + 1$) (from a nitrate). The contacts Cu(1)–N(15^I) and Cu(1^I)–N(15) could be regarded as a pairing between trimeric entities (see Figure 4).

In the coordination polyhedra of the three coppers of **2**, the apical position is occupied by an oxygen atom of a sulfate anion (Figure 3), with Cu–O(sulfato) distances of 2.26(1), 2.30(1), and 2.46(1) Å, which compare rather well with the axial distances observed in **1**. The way of coordination of the sulfate is an interesting structural aspect of this compound. The sulfato group binds axially two copper atoms of the same trimeric unit and a third copper atom from a different trimeric unit, thus building a chain of trimers and acting as tridentate bridging ligand. The intrachain interunit Cu⋯Cu' separation is 7.146(6) Å. As Figure 3 shows, the O(54) sulfato atom forms a hydrogen bond with the central

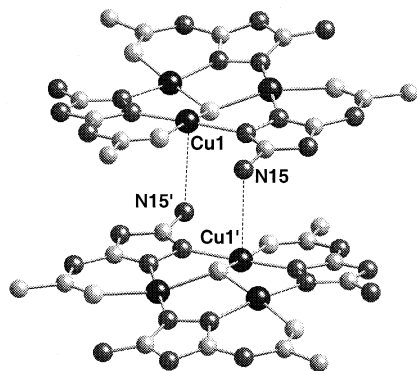


Figure 4. Diagram of **1** showing the pairing between trimeric units.

μ_3 -OH⁻ group [distances H(4)⋯O(54) = 1.763 (9) Å and O(4)⋯O(54) = 2.73(1) Å; angle O(4)–H(4)⋯O(54) = 168.6(6)°]. The IR spectrum of **2** exhibits bands of this unusual bridging-tridentate sulfate anion which are close to those reported for a C_{3v} symmetry:⁵² [$\nu_3(\text{SO}_4)$] 1140s–1110s; [$\nu_3(\text{SO}_4)$] 1066m–w; [$\nu_4(\text{SO}_4)$] 621m.

In **1** the trinuclear entities are packed in pairs (see Figure 4), with the respective $H(\text{OH}^-)$ pointing toward the other unit; the O(4)–O(4') distance is 7.819 Å. The shortest intertrimeric Cu⋯Cu' contact is 5.209 Å and the longest 11.257 Å.

A last structural feature, relevant for the discussion of the magnetic properties (see below), is that referred to the coplanarity of the ligand planes around each copper (as mentioned, defined by NN'OO'). The corresponding dihedral angles (deg) are as follows: in **1**, Cu(1)/Cu(2) = 18.8(2), Cu(2)/Cu(3) = 18.2(2), Cu(1)/Cu(3) = 11.2(2) (average: 16.1); in **2**, Cu(1)/Cu(2) = 24.3(3), Cu(2)/Cu(3) = 23.1(2), Cu(1)/Cu(3) = 15.0(2) (average: 20.8). These data will be considered in the next discussion.

Magnetic Properties

The temperature dependence of the $\chi_{\text{M}}T$ product (χ_{M} being the magnetic susceptibility per [Cu₃] entity) for complexes **1** and **2** is shown in Figures 5a and 5b, respectively. At room temperature the $\chi_{\text{M}}T$ values (0.72 and 0.75 cm³ mol⁻¹ K for **1** and **2**, respectively) are appreciably lower than those expected for three uncoupled $S = 1/2$ spins (ca. 1.2 cm³ mol⁻¹ K), and they decrease steadily with decreasing temperature. These curves clearly indicate that an intratrimer antiferromagnetic coupling is operating.

(a) Magnetic Behavior in the 90–300 K Temperature Range. In order to investigate the magnetic behavior of these trinuclear complexes, an isotropic Heisenberg–Dirac–van Vleck (HDVV) Hamiltonian formalism (eq 1) was used in a first approach.

$$\hat{H}_{\text{HDVV}} = -J_{12}\hat{S}_1\hat{S}_2 - J_{13}\hat{S}_1\hat{S}_3 - J_{23}\hat{S}_2\hat{S}_3 \quad (1)$$

Since the three copper atoms of the [Cu₃O] unit define a *quasi* equilateral triangle, the three Cu(II) ions can be considered equivalent, and so $J_{12} = J_{13} = J_{23} = J$. According

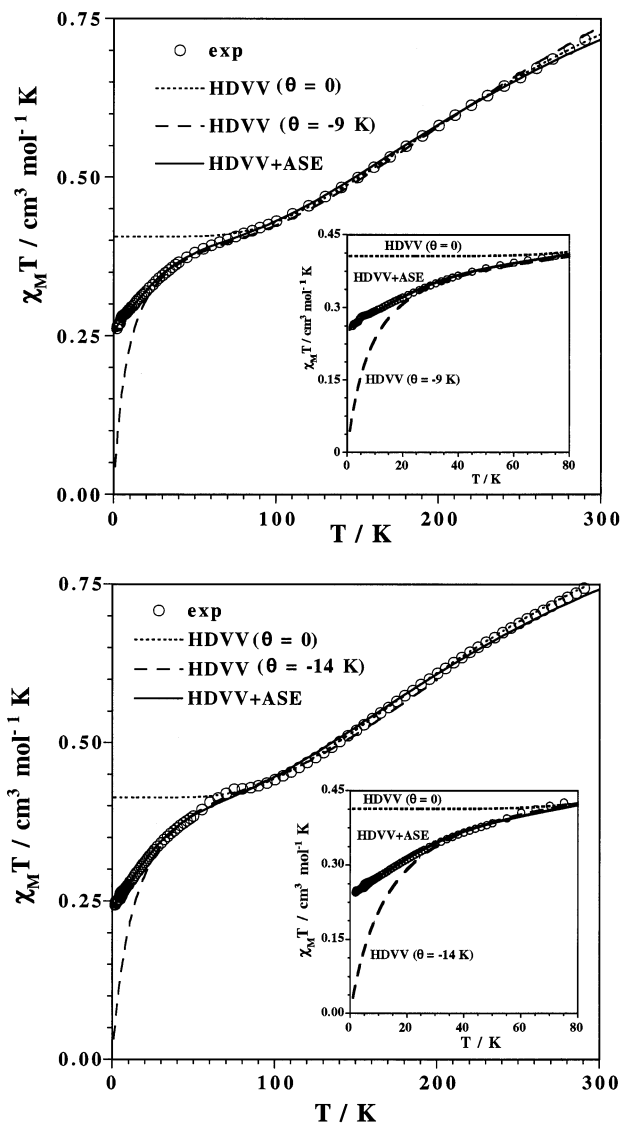


Figure 5. Thermal dependence of $\chi_{\text{M}}T$ for **1** (a) and **2** (b). The lines correspond to the best theoretical fit from different models (see text).

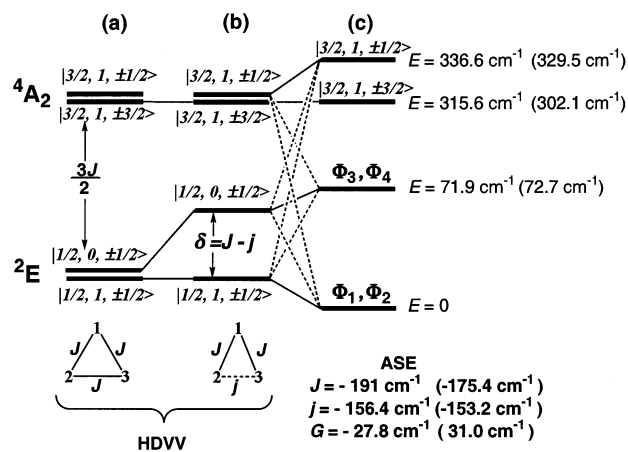


Figure 6. Energy levels for (a) an equilateral triangle system; (b) an isosceles triangle system; (c) the splitting–mixing of the b levels when the antisymmetric exchange (ASE) is operating. The calculated parameters for compounds **1** and **2** (in parentheses) are included.

(52) Nakamoto, K. *Infrared and Raman Spectra of Inorganic and Coordination Compounds*, 4th ed.; Wiley-Interscience Pub.: New York, 1986.

to this assumption, the experimental data could be fitted satisfactorily in the temperature range 90–300 K by using

Table 3. Coplanarity (Averaged Dihedral Angles between the Equatorial CuL₄ Ligand Planes) and *J* Values in {Cu₃(μ₃-O)(N-N)₃} Systems

compd ^a	av Cu/Cu' (deg) ^b	av Cu–O(H)–Cu' (deg)	– <i>J</i> (cm ^{–1}) ^c	ref
N–N (trz)				
1	16.1(2)	115.4(3)	195	this work
2	20.8(3)	113.7(4)	185	this work
3	25.3(2)	112.4(2)	198	7
4	24.4(1)	114.6(3)	191	7
5	21.1(2)	115.4(3)	198	7
6	26.2(3)	112.1(3)	191	5
N–N (pyr)				
7	27	114.5(1)	200 (ca.)	8
8	36	109.6(2)	140	51

^a trz = triazole; pyr = pyrazole. **1**, **2**, **3**, **4**, **5**: see text. **6** = [Cu₃(μ₃-OH)(hppt)₃(NO₃)₂]·4H₂O. **7** = [Cu₃(μ₃-OH)(pz)₃(μ₃-NO₃)(Hpz)₂](NO₃)·H₂O. **8** = [Cu₃(μ₃-OH)(pz)₃(py)₂Cl₂]. The triazole compound described by Virovets et al.⁶ has not been included because its structure presents strong disorder problems. ^b Coplanarity between the least-squares planes defined by [O(H), N(1), N(2), O]; average value calculated from the Cu1/Cu2, Cu2/Cu3, Cu1/Cu3 dihedral angles. ^c The *J* values from the literature have been modified according to the definition used in this paper (see eq 1).

the derived χ_{MT} equation, already reported.⁷ The best-fit parameters obtained are $J = -194.6 \text{ cm}^{-1}$ and $g = 2.08$ with $R = 1.8 \times 10^{-6}$ for **1**; $J = -185.1 \text{ cm}^{-1}$ and $g = 2.10$ with $R = 2.1 \times 10^{-6}$ for **2** (where R is the agreement factor defined as $\sum_i [(\chi_{MT})_i^{\text{exp}} - (\chi_{MT})_i^{\text{calc}}]^2 / \sum_i [(\chi_{MT})_i^{\text{exp}}]^2$).

As discussed earlier,⁷ several authors (Butcher et al.,⁴⁶ Angaroni et al.⁵¹) have correlated the magnitude of the magnetic coupling within the Cu₃O cluster with the coplanarity of the square-planar basal coordination planes of the copper atoms. Most of the trinuclear compounds containing a pyramidal Cu₃O(H) core described in the literature can be systematized in three groups depending on the type of peripheral bridge: those with an N,O (mainly from oxime–oximate ligands) bridge;^{44–48} those with an *N,N*-pyrazole bridge, with only three compounds reported;^{8,51} and those with an *N,N*-triazole bridge.^{5–7} In Table 3 we have compiled the information relevant to the N,N-bridged compounds. The results presented in this table support our first conclusion that the coplanarity, of the three basal planes of the interconnected CuL₅ coordination polyhedra, is not the determining factor in the magnitude of the exchange in this type of trinuclear clusters. While for compounds **1–6** the differences in coplanarity can be of 10.1° (ca. 39%), the maximum variation in the $-J$ values is of only 13 cm^{–1} (ca. 7%). In the literature data revised by Angaroni et al.,⁵¹ the highest coplanarity was reported for the N,O oxime compound [Cu₃(μ₃-O)L₃(ClO₄)₂] [HL = 1,2-diphenyl-2-(methylimino)ethanone-1-oxime] (**9**),⁴⁶ with interplanar angles of 27°, 20°, and 14° (with an averaged value of 20.3°); this compound has a $-J$ constant of 2000 cm^{–1}, and the related compound [Cu₃(μ₃-OH)L₃(ClO₄)](ClO₄) [HL' = 3-(phenylimino)butanone-2-oxime] (**10**),⁴⁶ with an average interplanar angle of 33°, exhibits a $-J$ constant of 244 cm^{–1}. In contrast, compound **1**, with an average dihedral angle of 16°, presents a $-J$ value of 195 cm^{–1}. So the electronic factors related to the nature of the ligand which affords the bridge are decisive. In this sense, in the more studied dinuclear doubly N,N bridged Cu(II) systems (for which there is a

proved dependence of *J* of the bridging angle), the *N,N*-pyrazole bridge has been shown to be more efficient in the exchange than the *N,N*-triazole bridge.^{2a,53} When the trinuclear systems are considered, the N,O peripheral bridges lead to higher *J* constants than the N,N peripheral bridges; more examples are needed to decide whether the *N,N*-triazole or the *N,N*-pyrazole bridge affords a better magnetic exchange.

(b) Magnetic Behavior below 90 K. The magnetic behavior of **1** and **2** below 90 K was more difficult to rationalize. With the aim of understanding the experimental data, let us first consider the energy spectrum deduced from Hamiltonian 1. For an equilateral triangle (*C*_{3*v*} point-group symmetry) the mentioned HDVV Hamiltonian leads to the eigenvalues given by eq 2,

$$E(S) = -\frac{J}{2}[S(S+1) - \sum_{i=1}^3 S_i(S_i+1)] \quad (2)$$

with

$$S = S_1 + S_2 + S_3 \quad \text{and} \quad S_1 = S_2 = S_3 = 1/2$$

The total spin, *S*, yields two spin doublets, with different spin intermediate $S' = 1$ and 0 ($S' = S_2 + S_3$), and a spin quartet. As derived from eq 2, the energy is determined uniquely by the total spin, *S*. Therefore, the ground state is degenerated with respect to the intermediate spin, S' (see Figure 6a).

If there is a distortion of the equilateral triangle to give an isosceles system (*C*_{2*v*} point-group symmetry), the application of the corresponding HDVV Hamiltonian (eq 3) leads to the eigenvalues given by eq 4.

$$\hat{H}_{\text{HDVV}} = -J(\hat{S}_1\hat{S}_2 + \hat{S}_1\hat{S}_3) - j\hat{S}_2\hat{S}_3 \quad (3)$$

$$E(S, S') = -\frac{J}{2}[S(S+1) - \sum_{i=1}^3 S_i(S_i+1)] - \frac{\delta}{2}[S'(S'+1) - \sum_{i=2}^3 S_i(S_i+1)] \quad (4)$$

where

$$S' = S_2 + S_3 \quad \text{and} \quad \delta = J - j$$

Now, the spin doublets are not degenerated and their energy depends on the value of S' . So, in the presence of an antiferromagnetic coupling, the low-lying spin states are a ground spin doublet (with $S' = 1$), an excited spin doublet (with $S' = 0$) at an energy of δ , and an excited quartet at $3J/2$ (see Figure 6b).

In both situations, equilateral or isosceles triangle, at low temperatures, for which only the ground spin doublet (or degenerated spin doublets) is thermally populated, the magnetic behavior should follow the Curie law. However, as shown in Figure 5, below 90 K the experimental χ_{MT} data lie below the theoretical Curie law values, which suggests

(53) Hanot, V. P.; Robert, T. D.; Kolnaar, J.; Haasnoot, J. G.; Reedijk, J.; Kooijman, H.; Spek, A. L. *J. Chem. Soc., Dalton Trans.* **1996**, 4275.

that other kinds of antiferromagnetic interactions are operative. The inclusion of an additional Weiss-like parameter, θ , which would account for possible intertrimer magnetic interactions (T replaced by $T - \theta$), was taken into account in the fitting, yielding θ values of 9–14 K. These large θ values are meaningless since, in light of the room temperature X-ray structure, intertrimer interactions should not be important due to the exceedingly long and unfavorable contacts between the trinuclear entities. In addition, a very significant feature is that, when temperature vanishes, the χ_{MT} data do not extrapolate to zero, as expected for intertrimer antiferromagnetic interaction (see dotted lines in the inset of Figure 5).

In conclusion, the HDVV model serves as a reliable basis for describing exchange clusters and transmits correctly the overall picture of spin states at high temperatures. However, serious discrepancies between the predictions of the theory and experimental data occur in the low-temperature region, where the structure of individual spin levels is important (as is the anisotropy). Therefore, it is necessary to go beyond the framework of the HDVV model.

Non-Heisenberg Exchange Contributions. According to the group-theory analysis of exchange multiplets, the spin quartet ($S = 3/2$) and the two degenerated spin doublets ($S = 1/2$ for an equilateral triangle in the HDVV model) correspond to the singlet 4A_2 and doublet 2E orbital, respectively.¹⁹ In this sense, the orbital degeneracy in the interacting ion system is the reason for the “accidental” degeneracy of the spin doublets.

The ground 2E term is split into two Kramer’s doublets, E' and $[A'_1 + A'_2]$ (representations of the C_{3v} double group symmetry), by spin–orbit interaction in first-order perturbation theory.¹⁹ The multiplet 4A_2 undergoes further splitting into two Kramer’s doublets in second order. So, the spin–orbit coupling mixes the different states yielding an anisotropic ground state. These features can be described as an effective interaction of the antisymmetric type. In principle, at low temperatures, the existence of an antisymmetric exchange may yield magnetic moment values lower than those expected for the Curie law in the HDVV model, which does not account for spin–orbit coupling. Another type of magnetic exchange that could reduce the magnetic moment of the ground state would be the biquadratic exchange,^{28,54} but it is not operative for local spins $S_i = 1/2$.

Antisymmetric Exchange Interactions. In order to explain the magnetic behavior of complexes **1** and **2** at low temperatures, the antisymmetric exchange (ASE) term was added to the above HDVV Hamiltonian:

$$\hat{H} = \hat{H}_{\text{HDVV}} + \hat{H}_{\text{AS}} \quad (5)$$

$$\hat{H}_{\text{AS}} = \sum_{ij} G_{ij} [S_i^x S_j^y - S_i^y S_j^x] \quad (6)$$

G_{ij} being the antisymmetric exchange vector ($G_{ij} = -G_{ji}$), which is usually taken as a parameter. For a trigonal symmetry, G_x and G_y vanish ($G_x = G_y = 0$) and the ASE is

axial ($G_{12}^z = G_{13}^z = G_{23}^z = G_z$). The effective antisymmetric exchange constant of the trimer, G , is proportional to the sum of the components of two-center interactions, G_{ij} . In the present case, $G = (G_z/6)\sqrt{3}$ and it is parallel to the trimer trigonal axis (z -axis).¹⁹

Diagonalization of the Hamiltonian H_{AS} leads to eq 7 for the four magnetic sublevels of the ground state in a trimeric complex:

$$E_{1,2}^{\pm} = \pm \left[G^2 + \left(\frac{g\mu_{\beta}H}{2} \right)^2 \pm g\mu_{\beta}H \cos(\alpha) \right]^{1/2} \quad (7)$$

where α is the angle between the direction of the applied field, H , and the z -axis. As a result of applying the ASE Hamiltonian, the 2E term (with two degenerated spin doublets in the HDVV model) is split into two Kramer’s doublets, separated by an energy gap of $2G$. The splitting has large effects on the magnetic susceptibility of the trimeric complexes; particularly, it yields a magnetic anisotropy in the ground state: the parallel susceptibility does not change significantly, while the perpendicular component is strongly affected at low fields and low temperatures, as derived from eq 8. At high temperatures ($kT \gg G$), χ_{\perp} tends to the limit

$$\chi_{\perp} = \frac{N\mu_{\beta}^2 g^2}{\sqrt{4G^2 + \mu_{\beta}^2 g^2 H^2}} \tanh \left(\frac{\sqrt{4G^2 + \mu_{\beta}^2 g^2 H^2}}{2kT} \right) \quad (8)$$

$\chi_{\perp} \rightarrow N\mu_{\beta}^2 g_{\perp}^2/4kT$; so does χ_{\parallel} , only differing in the g -factor (g_{\perp} instead of g_{\parallel}), and the system shows a magnetic behavior similar to that expected for an HDVV model (with no magnetic influence of the ASE). At low temperatures ($kT \ll G$), however, χ_{\perp} decreases rapidly, producing a temperature dependent magnetic anisotropy.

The complete Hamiltonian ($\hat{H} = \hat{H}_{\text{HDVV}} + \hat{H}_{\text{AS}} + \hat{H}_{\text{ZEEMAN}}$) has been used here to fit the experimental data in all temperature ranges. In a first approach, the structure was treated as an equilateral triangle and so, the relevant parameters were J , g_{\perp} , g_{\parallel} , and G . The experimental data did not satisfactorily reproduce the theoretical model at low temperature for either of the two complexes (**1** and **2**). This is not surprising because of the topology of the corresponding $[\text{Cu}_3(\text{OH})]$ units, which are not strictly equilateral triangles. Actually, the three copper ions are not equivalent and therefore the $[\text{Cu}_3(\text{OH})]$ groupings present a lower symmetry. In order to avoid overparametrization in the fitting process, a C_{2v} symmetry (slight distortion of the equilateral triangle to give an isosceles triangle) was assumed together with an identical g -factor for all three Cu(II) ions ($g_{1u} = g_{2u} = g_{3u}$, where $u = x, y, z$) and a common antisymmetric vector, G_{ij} , for all three pairs of interacting ions ($G_{12} = G_{13} = G_{23}$). Then, the relevant parameters were J , j , g_{\perp} , g_{\parallel} , and G , where $J = J_{12} = J_{13}$ and $j = J_{23}$. With this second approach, a very good fit of the experimental data was obtained in all temperature ranges (see solid line in Figure 5). The resulting best-fit parameters are $J = -191.0 \text{ cm}^{-1}$, $j = -156.4 \text{ cm}^{-1}$, $G = 27.8 \text{ cm}^{-1}$, $g_{\parallel} = 2.09$, $g_{\perp} = 2.00$ (fixed in the fitting process), and $R = 2.7 \times 10^{-6}$, for **1**; and $J = -175.4 \text{ cm}^{-1}$, $j = -153.2 \text{ cm}^{-1}$, $G = 31.0 \text{ cm}^{-1}$, $g_{\parallel} = 2.10$, $g_{\perp} = 2.10$

(54) Belinskii, M. I.; Kuyavskaya, B. Y.; Tsukerblat, B. S.; Ablov, A. V.; Kushkulei, L. M. *Koord. Khim.* **1976**, *2*, 1099.

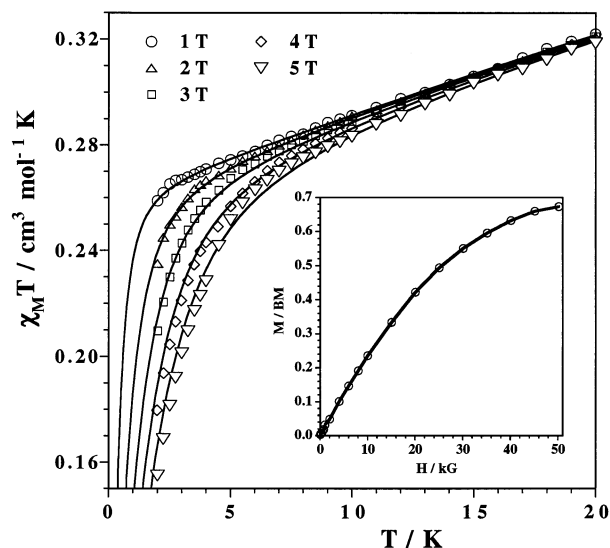


Figure 7. Thermal dependence of $\chi_M T$ for **1** at different applied fields in the low-temperature region. The inset displays the magnetization curve at 1.9 K for **1**. Solid lines represent theoretical curves (see text).

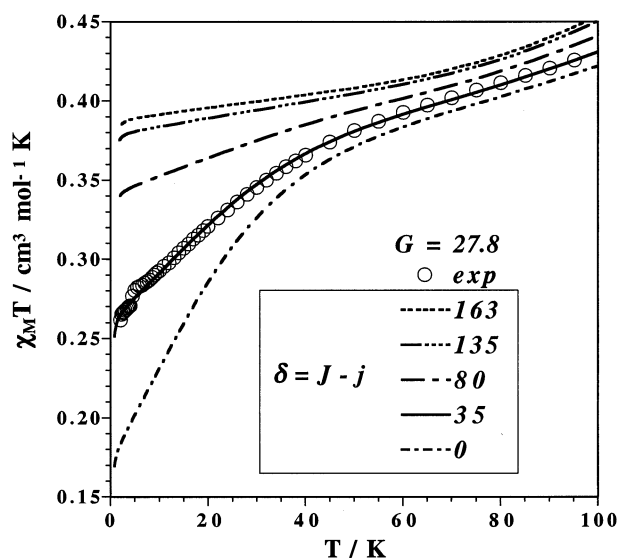


Figure 8. Experimental (for **1**) and calculated $\chi_M T$ curves for different δ values showing the influence of the distortion of an equilateral triangle toward an isosceles one when the antisymmetric exchange is operating (units for G , J , and j : cm^{-1}).

(fixed in the fitting process), and $R = 3.9 \times 10^{-6}$, for **2**. These parameters also reproduced satisfactorily the experimental polycrystalline $\chi_M T$ data at different fields as well as the magnetization curve. These results for compound **1** are depicted in Figure 7.

Figure 8 shows the effect of distortion of an equilateral triangle to give an isosceles structure when the antisymmetric exchange phenomenon is operating. The energy gap, $\delta = J - j$ (see Figure 6), can be used as the parameter which describes this distortion: $\delta = 0$ for an equilateral triangle, and the higher is δ , the larger is the rhombic distortion. When $\delta \gg G$, the system can be described by the HDVV model and the $\chi_M T$ curve follows the Curie law, as expected for the Heisenberg exchange. In the other limit case, when $\delta \ll G$, the antisymmetric exchange dominates the magnetic behavior, which is characterized by suppression of the

magnetic moment. The HDVV model can only be applicable if there is enough distortion as to suppress the anisotropy of the Zeeman splitting due to the antisymmetric exchange.

Although the necessity to introduce the antisymmetric exchange contribution in the study of the magnetic properties of symmetric trigonal complexes has long been considered,⁵¹ this interaction is rarely taken into account in the literature. To our knowledge, the complex $[\text{Cu}_3(\mu_3\text{-OH})(\text{pyridine-2-aldoxime})_3](\text{SO}_4) \cdot 10.5\text{H}_2\text{O}$, with a trigonal symmetry similar to that of compounds **1** and **2**, is the only trinuclear copper(II) complex whose magnetic properties have been interpreted from the antisymmetric exchange model. As mentioned earlier, a value of 6 cm^{-1} was obtained for its G parameter,²⁰ and this result was the first experimental observation of antisymmetric exchange in transition-metal complexes. Compounds **1** and **2** present higher G values (ca. 30 cm^{-1}), but Lines et al. reported, for the tetrameric complex $[\text{Cu}_4(\mu_4\text{-O})(\text{triphenylphosphine oxide})_4\text{Cl}_6]$, a G value of 28 cm^{-1} ,²¹ which is very close to those of **1** and **2**. The lack of literature data prevents further comparison and discussion of the data obtained in this work.

Finally, it would be interesting to perform magnetic measurements on single crystals of **1** and **2** in order to study the anisotropy, since the parallel and the perpendicular components of the susceptibility are significantly different. Attempts at growing single crystals of appropriate size are in progress.

Conclusions

Triazole derivatives with a suitable chelating substituent, such as Haaat and Haat, have proved to be interesting ligands since they allow one to isolate trinuclear Cu(II) complexes of the triangular type. In addition, with Haaat and under specific synthesis conditions, a unique chain of cyclic trinuclear Cu(II) complexes has been obtained. The products here described, compounds **1** and **2**, have been structurally characterized, and their magnetic properties have been studied. The magnetic parameters which result from the fitting ($-J$ ca. 190 cm^{-1}) reinforce the hypothesis that the coplanarity between the coordination basal planes of the interconnected Cu(II) atoms is not the decisive factor in the magnitude of the antiferromagnetic exchange within the Cu_3O cluster.

Antisymmetric exchange is expected to be operative in all spin-frustrated systems, but it has been largely neglected up to now. Considering the relevance of spin-frustrated systems in many biologically interesting compounds, it is of fundamental importance that experimental confirmation of its presence be finally achieved.

Acknowledgment. Dr. L. Lezama is very much acknowledged for assistance. The authors wish to thank the Spanish Ministerio de Ciencia y Tecnología through projects CICYT (PM-97-105-C02-01), CICYT (BQU2000-0219), FICYT (PR-01-GE-4), and CICYT (BQU2001-2928).

Supporting Information Available: Crystallographic data in CIF format. This information is available free of charge via the Internet at <http://pubs.acs.org>.

IC020179+